

RSC Advances

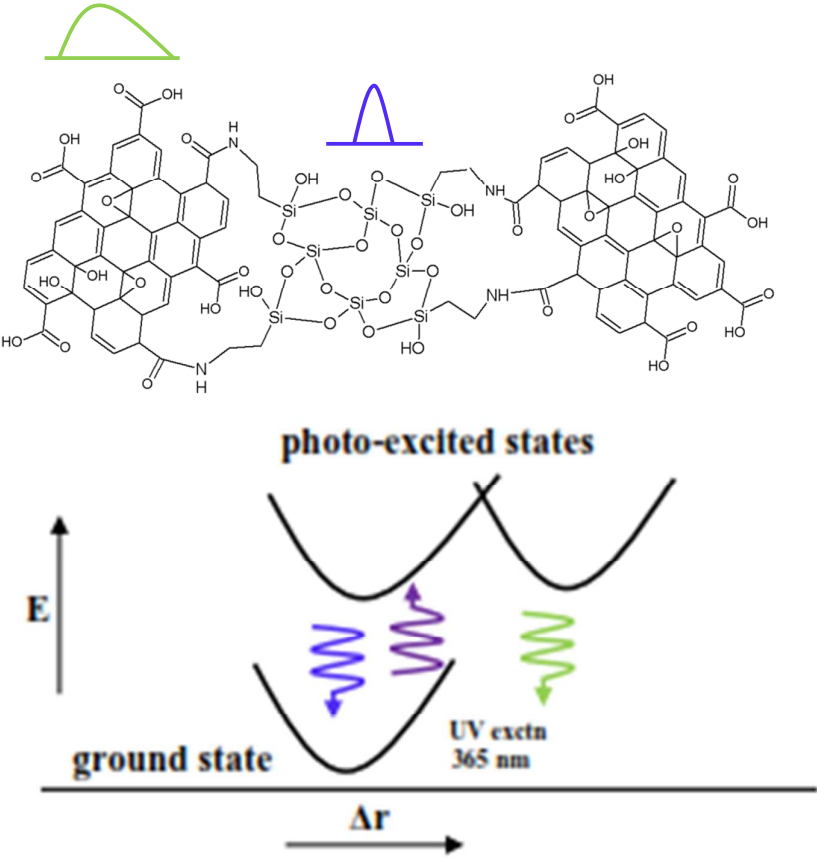


This is an *Accepted Manuscript*, which has been through the Royal Society of Chemistry peer review process and has been accepted for publication.

Accepted Manuscripts are published online shortly after acceptance, before technical editing, formatting and proof reading. Using this free service, authors can make their results available to the community, in citable form, before we publish the edited article. This *Accepted Manuscript* will be replaced by the edited, formatted and paginated article as soon as this is available.

You can find more information about *Accepted Manuscripts* in the [Information for Authors](#).

Please note that technical editing may introduce minor changes to the text and/or graphics, which may alter content. The journal's standard [Terms & Conditions](#) and the [Ethical guidelines](#) still apply. In no event shall the Royal Society of Chemistry be held responsible for any errors or omissions in this *Accepted Manuscript* or any consequences arising from the use of any information it contains.



Delocalization of electronic states in graphene oxide stabilised mesoporous silica nanoparticles revealed using photoluminescence

Naveen Chandrasekaran,^a Santhana Sivabalan,^a Ashwin Pratap,^b S. Mohan^a and
R. Jagannathan^{*a}

^a CECRI-CSIR, Karaikudi, Tamil Nadu, 630006. India.

^b Centre for Education, CSIR-CECRI, Karaikudi, Tamil Nadu, 630006 India.

*Corresponding Author E-mail: jags57_99@yahoo.com, naveen@cecricri.res.in.

Abstract:

Mesoporous silica aerogel obtained through a sol-gel process when surface treated with 2-D graphene oxide sheets reveal many fascinating features particularly, leading to multiple coordination complexes based on amide linkages. These could arise from reaction of amine groups present in the silica network and carboxylic acid groups in the edge planes of 2-D GO sheets as demonstrated and probed using photoluminescence spectra. New centres arising from the GO networking with silica nanoparticles seem to be more covalent (strong delocalization) as reflected from the asymmetric green luminescence bands.

Keywords: *Mesoporous silica nanoparticles, Graphene Oxide, Photoluminescence.*

1. Introduction:

Mesoporous solids attract great deal of interest in terms of diverse applications spanning a wide gamut starting from conventional sensing devices to recent biomedical, drug delivery systems [1-3]. With the advent of 1-D, 2-D nanoarchitectural designs, further augmentation in application scope has become feasible [4-6]. Microstructural information in these engineered mesostructures holds the key in eventually determining their characteristics and hence applications.

However, this class of mesoporous silica nanoparticles (MSNPs) suffers from porous structural instability, charge transport limitations etc., [7-10]. In order to address these inherent shortcomings of the MSNPs, chemists have been endeavouring several strategies, viz., impregnation of 2-D graphene oxide (GO) sheets having impressive surface area, mechanical and electrical properties can adequately address the shortcomings of pristine MSNPs. Notwithstanding extensive use of graphene oxide into the MSNPs for gainful applications, the information concerning microstructural modification following the graphene oxide networking with MSNP appears to be sparse.

Chemically modified graphene layers in nanoscale when treated with MSNPs bring about many fascinating properties *viz.*, superhydrophobicity, swift charge transport etc, to note a few [11, 12]. The enhancement in the performance of GO-MSNPs has been explained through chemical modification of organic functional groups chemically attached to GO and the subsequent microstructural modification occurring in the nano-hybrid phase. To our best knowledge, information concerning microstructural modification of MSNP with GO hybrid structure seems to be very limited. This may be because no powerful technique has been adopted to follow the microstructural changes confined to the molecular scale. This serves as motivation for us to employ photoluminescence (PL) spectra underlying electronic transition(s) confined to the molecular scale as a local probe to monitor structural changes of this technologically important nano-hybrid system. PL can be reliably used to image microstructural changes of the GO-MSNP hybrid without obscuring any relevant information. Furthermore, in this work we have also used another equally reliable tool to follow the microstructural changes *viz.*, selected area electron diffraction (SAED) results based on transmission electron microscopy (TEM).

2. Experimental Section:

2.1. Materials and Methods:

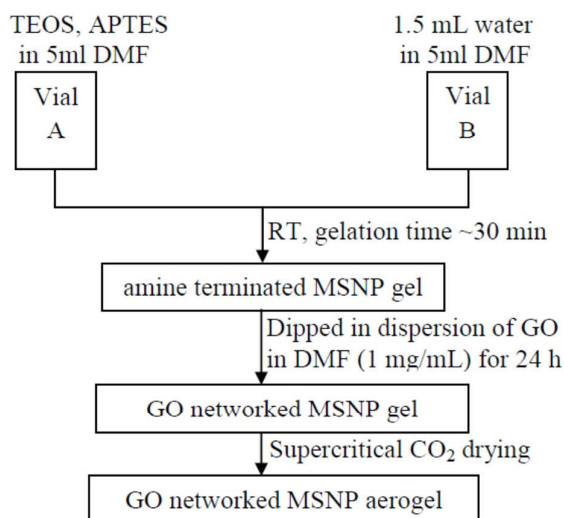
Starting material used in this work are, tetraethyl orthosilicate (TEOS) reagent grade, 98%, (3-Aminopropyl) triethoxysilane (APTES) 99% and N, N-Dimethylformamide (DMF) ACS Reagent, $\geq 99.8\%$, Acetone for HPLC, $\geq 99.8\%$ were used as obtained from Sigma-Aldrich. The amine modified and GO networked MSNP wet gels were transformed to aerogels using critical point drier (Model No: E3100, Quorum Technologies, Ltd). Infrared spectra on these samples in powder form were obtained using KBr pellets employing a Bruker Tensor 27 FT-IR spectrometer. Transmission Electron microscopy (TEM) and selected area electron diffraction (SAED) were obtained using Technai 20 G2 (FEI make). Photoluminescence spectra were recorded using JASCO FP8500 Spectrofluorometer (Model name: ESC-842, made in Japan). Polycrystalline X-ray diffraction pattern were obtained using a Bruker D8 Advance X-ray diffractometer with a Cu K α radiation ($\lambda=1.5418 \text{ \AA}$). The XRD data were refined using X'Pert Plus crystallographic analysis software with Rietveld capability. Thermogravimetric analysis was conducted in air with a simultaneous TGA/DTA TA Instruments Model SDT Q600 at a heating rate of $10^\circ\text{C}/\text{min}$.

2.2. Preparation of Graphene Oxide:

The GO used in this investigation was prepared following Hummer's method [13]. The synthesis procedure of GO started with slow addition of 100 mL concentrated H_2SO_4 to a mixture of 3 g graphite powder and 3 g NaNO_3 in a round bottomed flask; the temperature was maintained at 0°C using an ice bath under constant stirring. To the resulting black mixture, 12 g KMnO_4 was added slowly with vigorous stirring. After the complete addition of KMnO_4 , the mixture was maintained at 0°C under vigorous stirring. The temperature of the bath was increased and maintained at 35°C for 72 h. The brownish precipitate, thus obtained after this step was washed with copious amount of distilled water then the temperature was raised to 90°C . The solution obtained was diluted with 250 mL of distilled water which was kept standstill for 48 h before the addition of 10 mL of 30% H_2O_2 . Thus obtained graphene oxide was washed with 4% HCl followed by several washes with distilled water.

2.3. Preparation of GO modified silica aerogels:

Amine modified MSNP aerogels were prepared by mixing TEOS (11.7 mmol) and APTES (0.3 mmol) in 5 mL DMF taken in vial A and by subsequently adding 1.5 mL of water in 5 mL of DMF taken in vial B. The optimized gelation time of the amine modified MSNP aerogels was found to be 15 min. The obtained wet gels were washed using DMF (3 \times) for 24 h. The wet gels were dipped 1 mg of GO dispersed in 1 mL of DMF for 24 h. The wet GO networked gels were dried in an autoclave at supercritical conditions. The preparation of GO networked MSNP gels can be schematized as shown below.



Synthesis schematics of GO networked MSNP aerogel

3. Results and Discussion:

3.1. Morphology and networking of GO with MSNP:

Morphologies of GO, MSNP aerogel and GO networked MSNP aerogel are depicted in TEM electron micrographs (Figure 1a-c top panel) and their corresponding selected area electron diffraction patterns are given in bottom panels (Figure 1d-f). As can be seen from the micrographs, the GO used essentially adopts a two-dimensional sheet like structure while the MSNP revealed a porous structure. The GO sheets are much larger in dimension as compared to the pores of MSNP. Upon networking, we could see the porous MSNP is seen to be distributed over GO sheets: the amorphous nature of the MSNP whilst complexing with GO for 24 h done using transferring the MSNP gel into the sheets of GO dispersed in DMF resulted in nearly comparable particle morphology with distribution of GO sheets throughout the bulk.

Notwithstanding the size mismatch between the GO and pores of MSNP, there is clear possibility of chemical reaction between the carboxylic groups present in the edges of GO and amine present in the surface of MSNP. This might result in networking of GO with MSNP resulting in a new complex: essentially comprising dangling amine groups present in the silica network transforming to amide upon reaction with carboxylic acid present in GO. Turning to the structural examination using SAED patterns, we have that the GO revealed a crystalline spotty pattern while the MSNP revealed diffused rings suggesting amorphous nature. On the other hand, the SAED pattern of networked GO-MSNP aerogel leads to a totally complex picture. That is, the networked sample shows spotty ring characterizing polycrystalline nature of the sample in addition to twinning of diffraction spots (indicated using arrow). Twinning of SAED spots is quite possible in too closely spaced matching layered structures akin to a super-lattice structure [14, 15]. The occurrence of this kind of super-lattice structure can be visualized through considering amide linkage between MSNP and GO. The latter GO shows some kind of regular arrangement and expected to establish linkage with MSNP owing to the increased propensity for amide formation as modelled in Figure 2. Furthermore, to account for the occurrence of random spots in the SAED pattern (Figure 1.f): there is also clear possibility of having GO in reduced form (rGO) lacking any arrangement in orientation (Figure 2). The random occurrence of rGO can be rationalized in terms of ample scope for reduction of GO when present in DMF solvent medium, an established reducing agent. [16]

Also, in view of superficial nature limited to the surface of the MSNP, chemical reaction of GO networking into MSNP is expected not to alter the inter-planar spacing of the pore structure of the MSNP. However, we do get clear evidence in X-ray diffraction results manifesting in a weak structure corresponding to GO appearing in the networked MSNP aerogel (marked using bold arrow in Figure 3) in addition to marginal change in the d-spacing of the dominant line.

In order to identify probable functional groups attached to the MSNP aerogel, FTIR spectra of APTES, GO, MSNP aerogel and networked MSNP aerogel samples have been recorded as depicted in Figure 4. FTIR spectra of APTES showed their characteristic peaks at 1136 cm^{-1} and 995 cm^{-1} which can be assigned to Si-O-H and Si-O-Si groups. The presence of peaks at 1612 cm^{-1} , 2968 cm^{-1} and 3401 cm^{-1} can be ascribed to the δ (NH_2), ν (CH) and ν (N-H) vibrations respectively. FTIR spectra of the as-prepared GO sheets displayed their characteristic ν (C=O) peak at 1708 cm^{-1} , ν (C=C) peak at 1567 cm^{-1} , δ (OH) deformation vibration at 1370 cm^{-1} , ν (C-OH) vibration at 1224 cm^{-1} , ν (C-O) vibration at 1037 cm^{-1} and a broad intense OH peak at 3400 cm^{-1} .

On the other hand, formation of new peaks in the FTIR spectra of GO-MSNP aerogel at 1541 cm^{-1} (ν C=C) and 3321 cm^{-1} (ν NH) can be attributed to the presence of π bonds in GO and amide linkage formed *via* the reaction of carboxylic acid groups present in the GO and dangling amines in the MSNP aerogel respectively. The epoxide ν (C-O) peak present in GO completely disappeared in the networked aerogels which may be ascribed to the ring opening of epoxide by amine functionalities present in the MSNP gel. These results confirm the successful networking of GO onto the surface of MSNP gel.

In order to assess the intake of GO onto the surface of MSNP, thermogravimetric analysis have been carried out for GO sheets only, MSNP and networked aerogels. Accordingly, as shown in Figure 5, it turns out that at 800°C , GO sample showed almost 100% weight loss, whereas, the MSNP and networked aerogels showed weight loss of 74.76% and 65.5% respectively which clearly indicates ~8% of GO onto MSNP aerogels.

3.2. Delocalization of network revealed using luminescence bands

Luminescence glow and luminescence emission band(s) following photo-excitation process results from relaxation of excited electronic state(s) usually limited to the first coordination sphere around the luminescent electron centre(s). Here, photochemical activity of the pristine

MSNP aerogel is observed as intense blue-violet glow. The glow and the luminescence emission band spectra of the pristine system with $\lambda_{\text{max}} = 412$ nm (labelled as PB in Figure 6 (top panel)) can be well explained: moderately intense single Gaussian emission band might suggest a unique luminescent centre involved in this process. The pristine system earlier labelled as MSNP can be chemically visualized in terms of amine terminated silica.

Turning to describe the photochemical process of the networked aerogel: the networked system shows bright yellowish-green glow associated with complex emission bands. The complex emission spectra having several bands including the PB indicate the presence of multiple coordination complexes generated consequent to networking. Additional emission bands of the networked system lies at longer wavelength in the green-yellow region with unduly broadened spectral widths (labelled as GB in Figure 6 (bottom panel)). With the knowledge of Stokes shift for the pristine band PB showing nearly comparable value of $\sim 4000 \text{ cm}^{-1}$ in both cases of pristine and networked aerogel systems, we can estimate a nearly comparable electron-lattice coupling strength (also referred as Huang-Rhys factor) [17] which works out to be 2 for both the systems. On the other hand, the estimate of electron-lattice coupling strength concerning the spectral data corresponding to the band GB at longer emission wavelength suggests a higher value of 3-4. Furthermore, the long wavelength emission band having a large band width seems to stem from a centre which may have different origin. This can be attributed to totally different kind of electron center(s). Summing up these photo-luminescence results, we can predict the presence of atleast two kinds of centres, *viz.*, PB centre attributed to pristine emission band and another kind showing large band width to a delocalized centre GB. The origin and occurrence of these two kinds of photoactive electron centres can be visualized in terms of the chemical structure of the pristine system and the subsequent modification which ensue consequent to GO networking.

Describing the details of the chemical structure of the pristine mesoporous system: this mesostructure has Si-O-Si strong linkage (center I) along with weak Si-O-H linkage accompanied with dangling amine groups (center II) comprising lone pair of electrons. The first kind of center arising through Si-O-Si linkage can lead to a localized electronic center not undergoing any strong deformation even upon networking as can be seen through nearly similar emission bands for both the pristine and the networked systems assigned as PB. On the other hand, the second kind of center occurring only in the case of networked system might stem from a more delocalized center (characterized by large spectral band width nearly two fold as that of PB) as a result of amine to amide transformation as outlined earlier. Also,

the presence of lone pair might facilitate intense photo-absorption followed by luminescence emission in the UV-Visible region with large band width due to strong delocalization of photo-excited electronic states characterized. This indeed is the case, with the luminescent glow and the associated emission bands undergoing drastic modification upon networking with GO, namely, the blue glow turns green-yellow and the emission band becomes more complex acquiring multiple bands along with the original emission band as outlined in Figure 7. Strong delocalization of photo-excited state should result from drastic change in the coordination geometry of chemical complexes. Furthermore, higher value of electron lattice coupling strength is another indicator of stronger coupling experienced in the complex, *viz.*, networked GO-SiO₂. In this context, it is pertinent to note that amide complexes can lead to intense luminescence glow in the visible region [18, 19].

4. Conclusions:

Summing up the results, using a facile sol-gel process based on hydrolysis and condensation of TEOS and APTES, GO modified MSNP aerogel exhibiting fascinating properties have been synthesized. Upon modification, the GO-MSNP aerogel results in more complex electron centers which can be explained through amide linkages. Attempts to characterize these complexes using photoluminescence, FTIR techniques facilitated insights on different complexing features of GO networked MSNPs. Notably, the carboxylic acid groups in oxidized graphene sheets has strong propensity to react with the dangling amine groups present in the MSNP aerogel eventually forming more asymmetric amide complex. This would facilitate intense photochemical activity essentially comprising strong delocalized electronic transitions in the energy regime of a few eV as reflected from the green emission band of large, asymmetric width. Electron transfer type charge transfer reactions would increase manifold in presence of more conducting graphene sheets. Basically the GO seems to occur in two forms *viz.*, (i) GO-MSNP super-lattice structure and (ii) randomly distributed reduced GO. The asymmetric green fluorescence emission band resulting from GO networking with MSNP characterized by large electron-lattice coupling strength indicates a strong delocalization of the excited electronic states. This may in turn suggest a stronger covalency prevailing in the GO networked MSNP system over the pristine silica system which may be useful to account for the enhanced sensing, charge transfer properties meriting fascinating applications.

Acknowledgements

The authors thank CSIR-CECRI for the financial support from 12th five year project no: CSC0114.

References:

- 1 Y. Huang, S. F. Y. Li, *J. Electroanal. Chem*, 2013, **690**, 8-12.
- 2 S. Sreejith, X. Ma, Y. Zhao, *J. Am. Chem. Soc.*, 2012, **134**, 17346- 17349.
- 3 X. Yang, X. Zhang, Z. Liu, Y. Ma, Y. Chen, *J. Phys. Chem. C.*, 2008, **112**, 17554-17558.
- 4 R. K. Joshi, J. J. Schneider, *Chem. Soc. Rev.*, 2012, **41**, 5285-5312.
- 5 D. Rollison, *Science*, 2003, **299**, 1698-1701.
- 6 C. A. Morris, M. L. Anderson, R. M. Stroud, C. I. Merzbacher, *Science*, 1999, **284**, 622-624.
- 7 N. Leventis, *Acc. Chem. Res.*, 2007, **40**, 874-884.
- 8 U. F. Ilhan, E. F. Fabrizio, L. McCorkle, D. A. Scheiman, A. Dass, A. Palczar, M. A. B. Meador, J. C. Johnston, N. Leventis, *J. Mater. Chem*, 2006, **16**, 3046-3054.
- 9 J. P. Randall, M. A. B. Meador, S. C. Jana, *J. Mater. Chem A*, 2013, **1**, 6642-6652.
- 10 J. H. Park, L. Gu, G. V. Maltzahn, E. Ruosalhti, S. N. Bhatia, M. J. Sailor, *Nat. Mater.*, 2009, **8**, 331-336.
- 11 C. Gomez-Navarro, R. T. Weitz, A. M. Bittner, M. Scalori, A. Mews, M. Burghard, K. Kern, *Nano Lett.*, 2007, **7**, 3499-3503.
- 12 M. J. Allen, V. C. Tung, R. B. Kaner, *Chem. Rev.*, 2010, **110**, 132-145.
- 13 M. Li, J. Ding, J. Xue, *J. Mater. Chem. A.*, 2013, **1**, 7469 - 7476.
- 14 H. Xu, P. R. Buseck, M. Carpenter, *American Mineralogist*, 1997, **82**, 125-130.
- 15 Y. Nakajima, P.H. Ribbe, *American Mineralogist*, 1981, **66**, 142-147.

- 16 S. Dutta, C. Ray, S. Sarkar, M. Pradhan, Y. Negishi, T. Pal., *ACS Appl. Mater. Interfaces.*, 2013, **5**, 8724-8732.
- 17 G. Blasse, *Prog. Solid. St. Chem.*, 1988, **18**, 79-171.
- 18 S. C. Nunes, V. D. Z. Bermudez, J. Cybinska, A. S. Ferreira, L. D. Carlos, M. M. Silva, M. J. Smith, D. Osrovskii, J. Rocha, *J. Mater. Chem.*, 2005, **15**, 3876-3866.
- 19 A. Gomaez-Suarez, D. J. Nelson, D. G. Thompson, D. B. Cordes, D. Graham, A. M. Slawin, S. P. Nolan, Belisten. *J. Org. Chem.*, 2013, **9**, 2216-2223.

Figures:

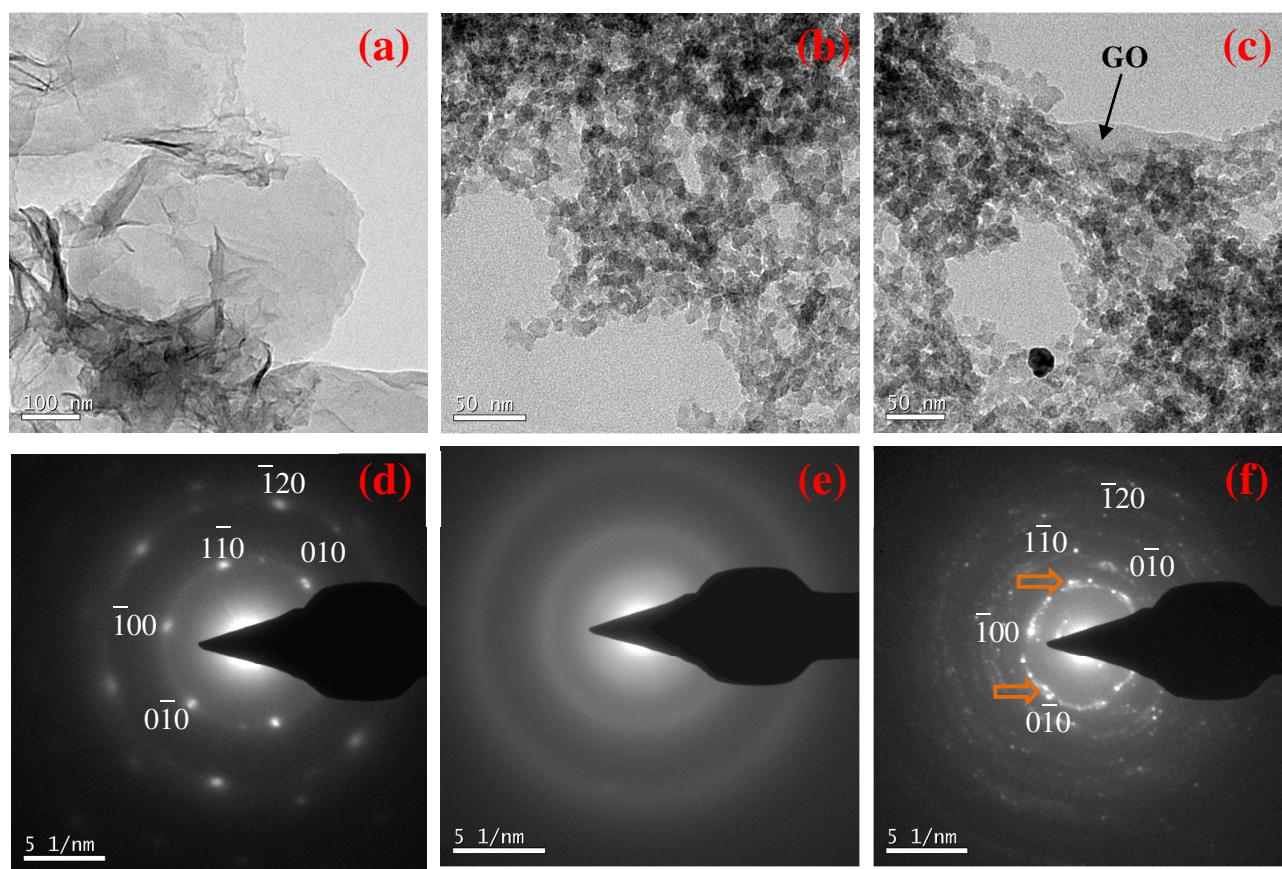


Figure. 1 TEM images (top panels) depicting particle morphology of (a) GO, (b) MSNP aerogel, (c) GO-MSNP aerogel. Bottom panels: corresponding SAED patterns of (d) GO, (e) MSNP aerogel, (f) GO-MSNP aerogel.

(\Rightarrow illustrates twinning of SAED spots in GO-MSNP aerogel)

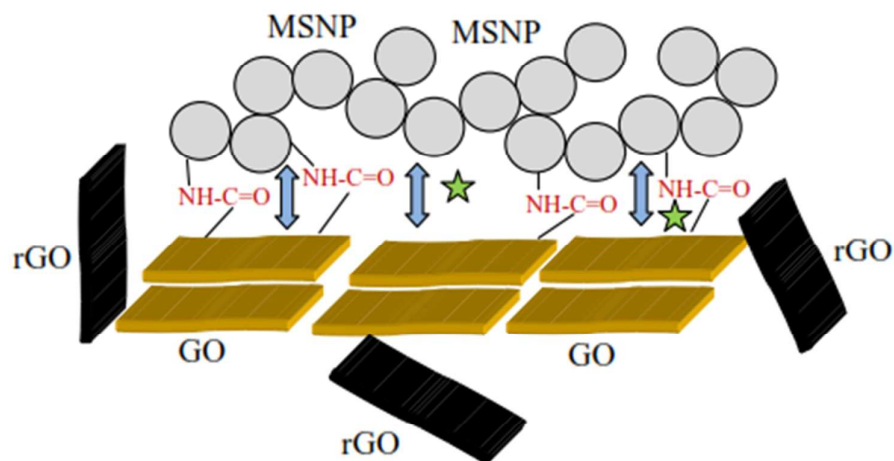



Figure 2. Schematics illustrating super-lattice formation (denoted by double headed arrow with ) through amide linkage between MSNP and GO. rGO denotes random occurrence of reduced GO sheets.

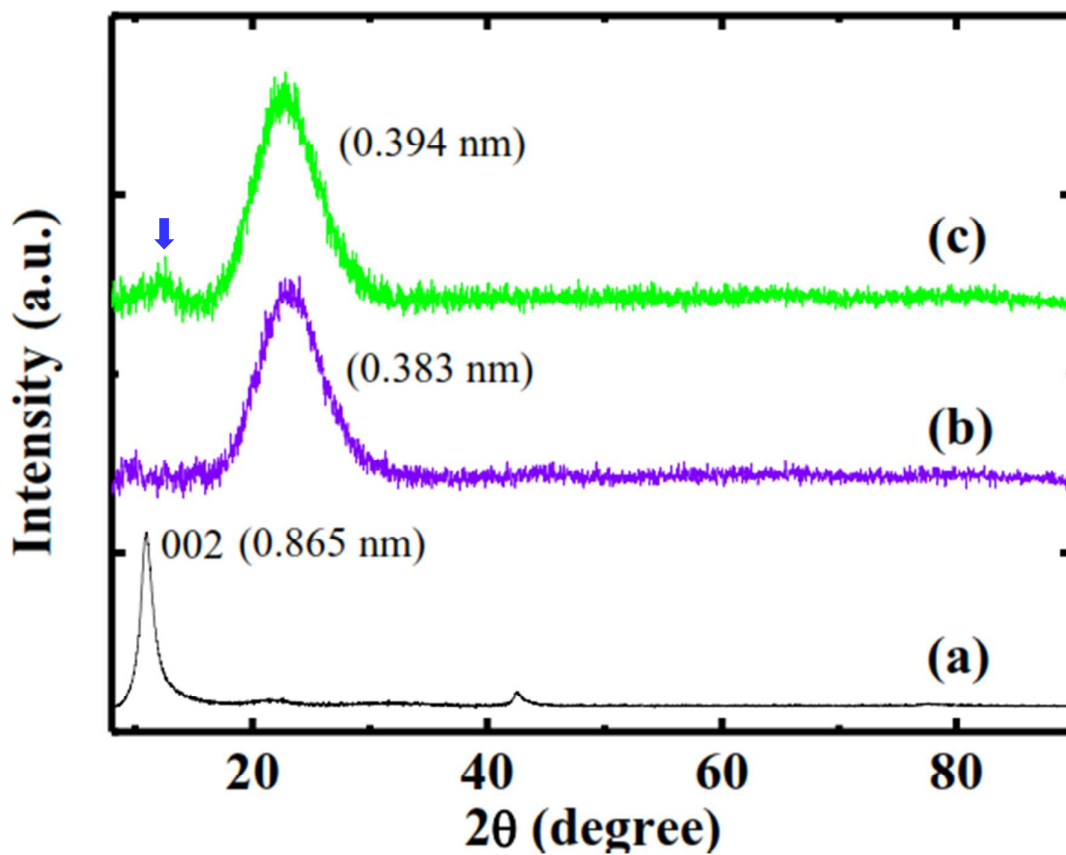


Figure 3. XRD patterns of (a) GO, (b) MSNP aerogel, (c) GO-MSNP aerogel (↓ indicates modified GO position in GO-MSNP aerogel).

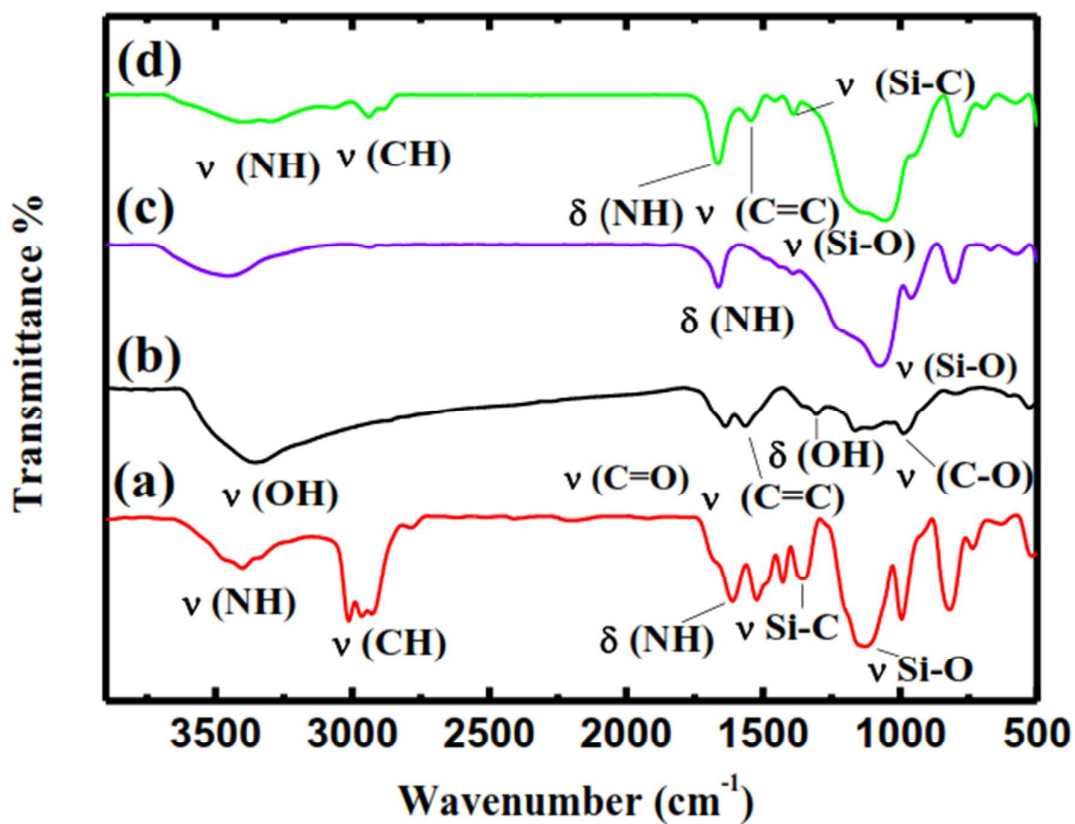


Figure 4. FTIR spectra of (a) APTES (b) GO, (c) MSNP aerogel, (d) GO-MSNP aerogel.

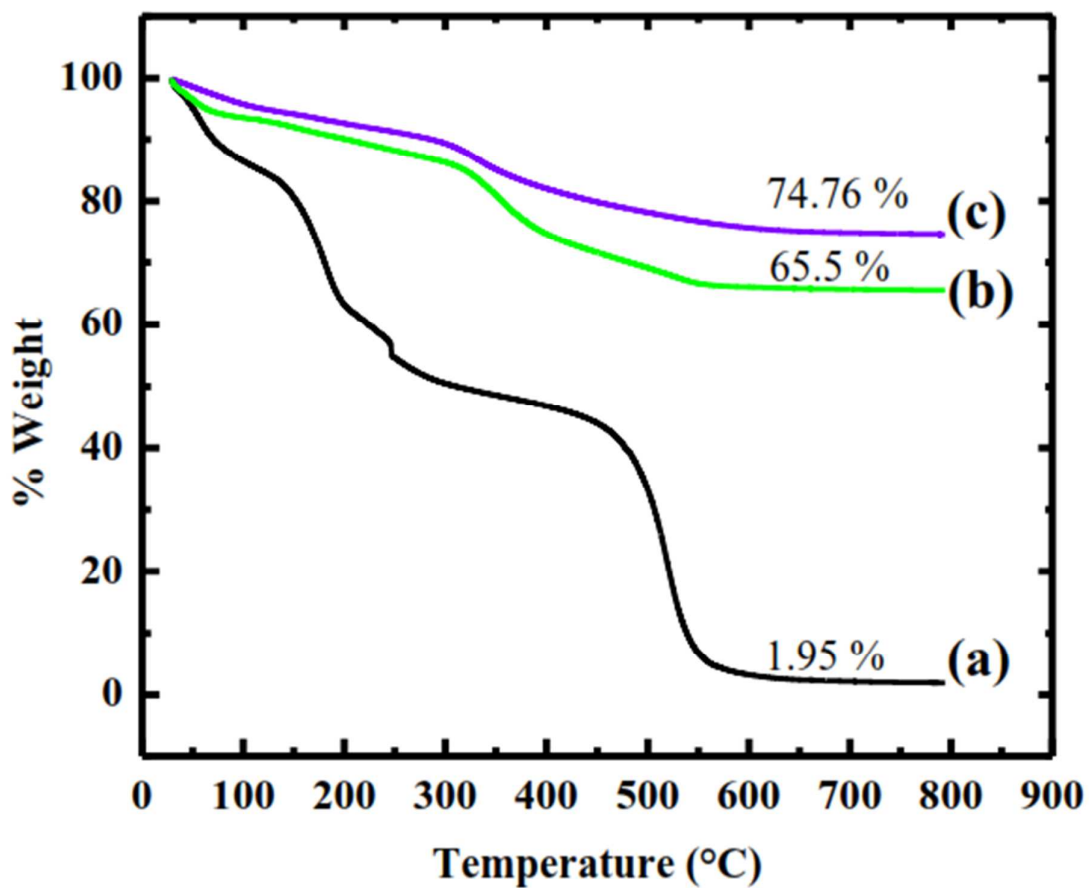


Figure 5. Thermogravimetry traces of (a) GO, (b) MSNP aerogel, (c) GO-MSNP aerogel.

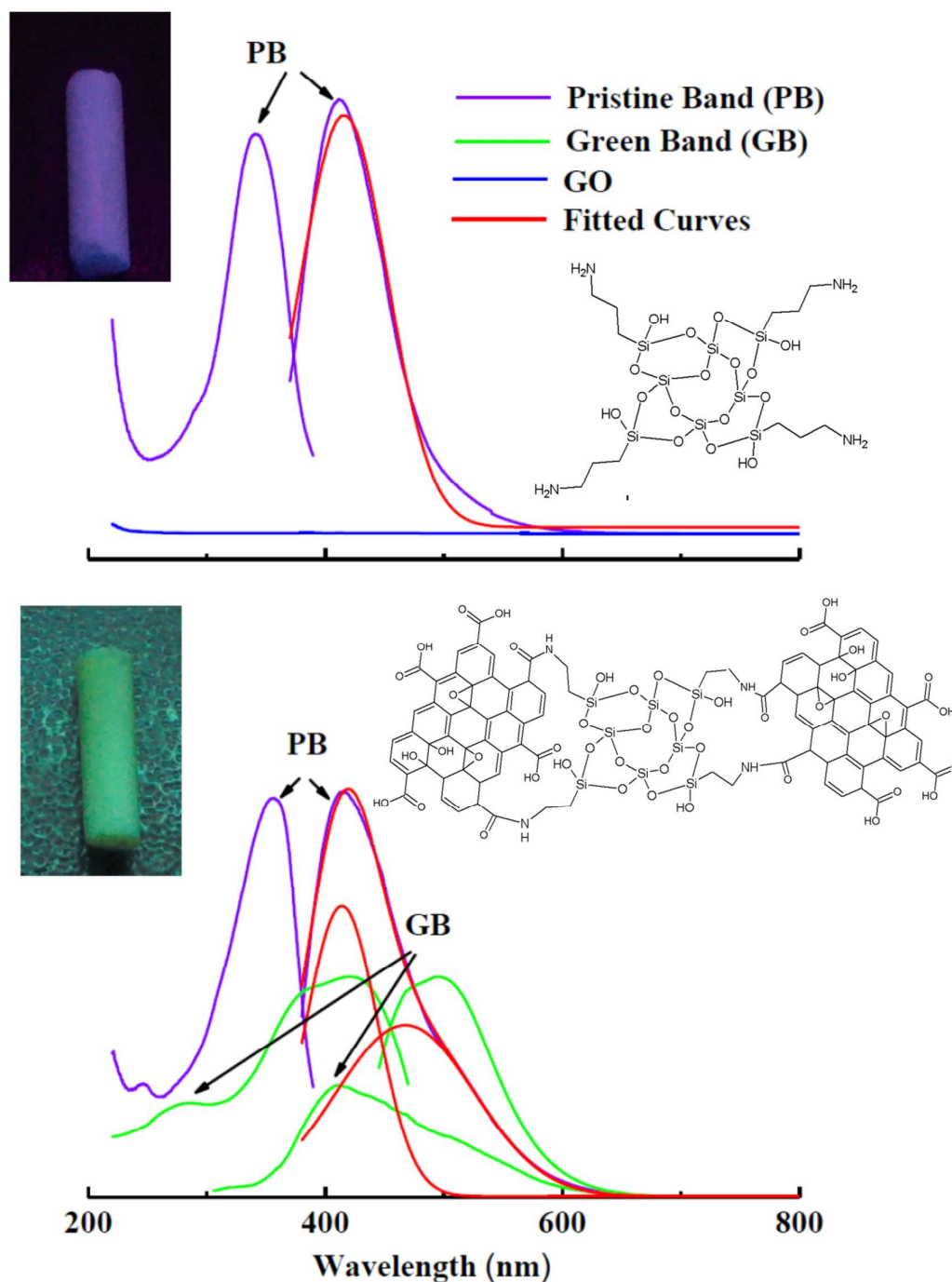


Figure 6. Photoluminescence (PL) excitation, emission spectra of MSNP aerogel (fitted curve included), GO (top), GO-MSNP aerogel (bottom). Insets: blue-violet glow for MSNP aerogels (top panel) and green-yellow glow for GO-MSNP aerogel (bottom panel) upon long UV (365 nm) excitation on the powdered samples. PL emission spectra were recorded at 300 K monitoring respective excitation and emission maxima.

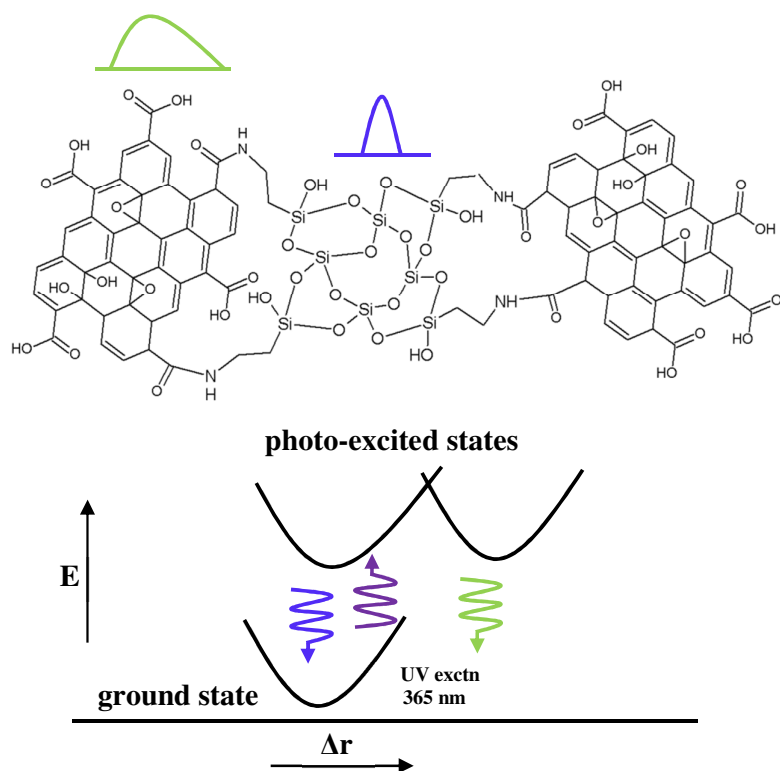


Figure 7. Schematics explaining the occurrence of PB-blue (localized) and GB-yellowish-green (delocalized) emission bands in GO-MSNPs aerogel.